# Supplementary Information

## The hippocampal CA3 area implements sequence learning of discontinuous episodes

Running title: Sequence learning in the CA3

*Authors:*

Kisang Eom[1,2,3#], Yujin Kim[1,2#], Hyoung-Ro Lee[1], Yolguk Lee[2], Young-Eun Han[1], Jiwoo Shin[1], Jae Sung Lee[4], Jung Ho Hyun[3], Alan J Park[1], Suk-Ho Lee[1,2,*]

*Affiliations:*

[1]Department of Physiology, Seoul National University College of Medicine, 103 Daehak-ro, Jongno-gu, 03080, Seoul, Republic of Korea.
[2]Department of Brain and Cognitive Science, Seoul National University College of Natural Science, 103 Daehak-ro, Jongno-gu, 03080, Seoul, Republic of Korea.
[3] Department of Brain Sciences, DGIST, Daegu 42988, Republic of Korea
[4]Howard Hughes Medical Institute, Beth Israel Deaconess Medical Center, 330 Brookline Ave., Boston, MA 02215, USA.

[#]These authors contributed equally.

*Correspondence: Suk-Ho Lee: leesukho@snu.ac.kr

## Supplementary Discussion

*Conditions for hetero-association and trans-ensemble excitation under the CA3 network of a rat scale*

While activation of the first ensemble is triggered by external PP inputs in Fig. 7E, sequential activation of the rest ensembles is accomplished by inputs from seed firing of pyramidal cells (PCs) of the preceding ensemble ($M_i$*, called a bridge subset) that are strongly connected to a given ensemble ($M_{i+1}$). In order for activation of PCs in a bridge subset, $M_i$*, to activate all the PCs in the next ensemble ($M_{i+1}$) through a pattern completion process, the seed firings of PCs in the bridge subset should regenerate firings of at least a PC in the next ensemble ($M_{i+1}$).

To this end, first we would calculate the minimal number of synchronous A/C-EPSPs for a postsynaptic PC to be fired, which is denoted as $N_{thr}$. For simplicity, we set the voltage gradient for AMPA receptor current ($\Delta E = V_m - E_{rev}$) constant at 50 mV, the value in the middle of RMP (=-60 mV)[1] and the threshold voltage for an action potential (AP = -40 mV). The voltage response [v(t)] to an A/C-EPSC input, $G_s \Delta E \exp(-t/\tau_s)$, is

$$v(t) = J\,[\exp(-t/\tau_m) - \exp(-t/\tau_s)],$$

where $J = (G_s/G_m)\,\Delta E / (\tau_m/\tau_s - 1)$. When $G_m$ = 5 nS[1], $G_s$ = 1 nS, $\Delta E$ = 50 mV, $\tau_m$ = 60 ms and $\tau_s$ = 10 ms[2], this EPSP has a voltage peak of 1.6 mV at $T_{peak}$ of 21.5 ms from the onset of EPSC (*Appendix*). Assuming that all PCs in an ensemble fire within a gamma cycle or 20 ms [3], the voltage increment ($\Delta V_k$) caused by $k$ EPSPs arriving within 20 ms is roughly close to 1.09 $k$ mV (*Appendix*). Paired recording of CA3-PCs revealed that mean $G_s$ at A/C synapses is 0.5 nS [2]. In the above calculation, we assumed that the synaptic connections between PCs within the same ensemble are two times stronger than this baseline value (*i.e.* 1 nS). When the expected $\Delta V_k$ is 1.09 $k$ mV and the threshold potential ($V_{thr}$) is 20 mV higher than the RMP, the minimal number of synchronous A/C-EPSPs for a postsynaptic PC to be fired ($N_{thr}$) is calculated as 19.

If $n$ PCs in an ensemble are fired by PP inputs (called 'recipient PCs'), and the connectivity is $p$ (=0.02)[2], the probability that other PCs receive excitatory inputs from more than $k$ PCs is :

$$P_M(k, n, p) = \Sigma_{i=k..n}\, C(n, i)\, p^i\, (1-p)^{n-i} \quad .$$

$P_M(k, n, p)$ can be evaluated from $1 - F(k, n, p)$, where F is a binomial cumulative distribution function (cdf). To activate all PCs in an ensemble through pattern completion, PCs fired by extra-ensemble input should activate at least one other PC in the same ensemble.

When an ensemble is comprised of $N_A$ PCs, we would like to find minimal $n$ such that at least one non-recipient ensemble PC receives A/C inputs from more than $N_{thr}$ recipient PCs. Assuming that the total number of CA3 PCs is 2 x $10^5$ and 5% of total CA3 PCs comprise an ensemble [4, 5], $N_A$ = 10000, and we can read $n$ from the plot of $(N_A - n) \times P(N_{thr}, n)$ at the point where a y-value just exceeds one, resulting in $n$ of 380 (*black dot* in Figure D1). This means that firing of about 380 PCs within a gamma cycle is needed to trigger regenerative firings of whole ensemble PCs encoding the next event through pattern completion.

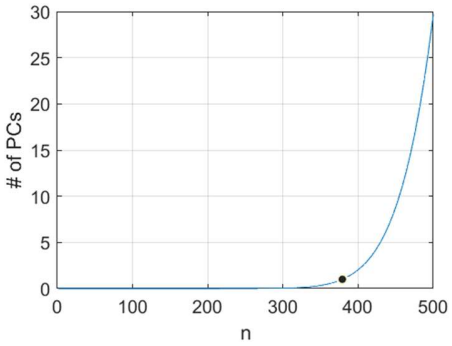


Figure D1, The plot of $(N_A - n) \times P(N_{thr}, n)$ as a function of $n$. $N_A$, ensemble size (=10000); $N_{thr}$, minimal number of presynaptic PCs to overcome AP threshold (=19); $n$, size of a bridge subset.

The next question is how many PCs in $M_i$* are required to activate 380 PCs in the next $M_{i+1}$ subset. When $n$ and $N_A$ PCs comprise of $M_i$* and $M_{i+1}$ subset, respectively, regenerative pattern completion can be triggered in the $M_{i+1}$ when $N_A\, P(N_{thr}, n, p) > 380$. As $n$ increases, the binomial distribution, $P(k, n, p)$, can be approximated to a normal distribution with its mean of $n\, p$ and variance of $n\, p\, (1-p)$. Thus,

$$P(k, n, p) = 1 - F(k, n, p) \cong 1 - \Phi[(k - np) / \sqrt{(n\, p\, (1 - p))}]$$

, where $\Phi$ is a cumulative standard normal distribution function. We can find $n$ such that $N_a P(N_{thr}, n) > 380$ from the equation:

$$\Phi^{-1} (1 - 380/N_A) = (k - n p) / \sqrt{(n p (1-p))},$$

where $\Phi^{-1}$ is an inverse function of normal cdf, and we have $n = 637$, suggesting that about 6.4% PCs of an ensemble should undergo LTP-IE in order for hetero-association of two different memory ensembles and sequential retrieval of a series of sequence memory ensembles. It should be noted that, in this calculation, we assumed that each ensemble cells fire only once in a gamma cycle, and did not consider the effects on membrane potential exerted by burst firing of ensemble cells, the conductance changes through NMDA and GABA receptors and background A/C synaptic inputs arriving from other ensemble PCs.

*Plausibility for all the CA3 principal cells to receive ensemble inputs from EC via PP*

There are 4000 PP synapses in a CA3 PC in average [4]. The proportion of Arc(+) neurons in the entorhinal cortex (EC) is c.a. 20%, and higher (40%) for CA3-projecting EC cells [6]. We assume parsimoniously 10% of EC cells are recruited for a memory ensemble. Assuming that 1) the number of CA3-projecting neurons in the EC is $2 \times 10^5$ ($N_{EC}$); 2) 10% of these neurons ($\alpha_{EC}$) participate in a neuronal ensemble, and 3) each of CA3 PCs receives synaptic inputs from 4000 EC neurons ($F_{EC}$) [4], the probability that a CA3 PC receives synaptic inputs from $X_{pp}$ EC ensemble cells can be calculated from a following hypergeometric probability density function as shown in O'Reilly and McClelland (1994) [7]

$$P(x_{PP}) = C(\alpha_{EC} N_{EC}, x_{PP}) C(N_{EC} - \alpha_{EC} N_{EC}, F_{EC} - X_{PP}) / C(N_{EC}, F_{EC})$$

, where C(n,k) is $k$-combinations from a set comprised of $n$ elements. $P(X_{pp})$ is shown in Figure D2 when $N_{EC} = 2 \times 10^5$, $\alpha_{EC} = 0.1$, and $F_{EC} = 4000$. This hypergeometric distribution can be approximated to a Gaussian distribution with a standard deviation of 18.8 [$= \sqrt{F_{EC} \alpha_{EC} (1- \alpha_{EC}) (1 - F_{EC}/N_{EC})}$] centered at 400 ($= \alpha_{EC} F_{EC}$). Thus, most CA3 PCs receive from at least 300 EC ensemble

cells [$P(X_{PP} < 300) = 1.8 \times 10^{-8}$]. On the other hand, similar calculation for $P(X_{MF})$ under the parameter set for MF-CA3 synapses ($N_{DG} = 2 \times 10^6$, $\alpha_{DG} = 0.01$, and $F_{DG} = 40$) results in a highly skewed distribution similar to the assumption of our simulation (Fig. 6Bb).

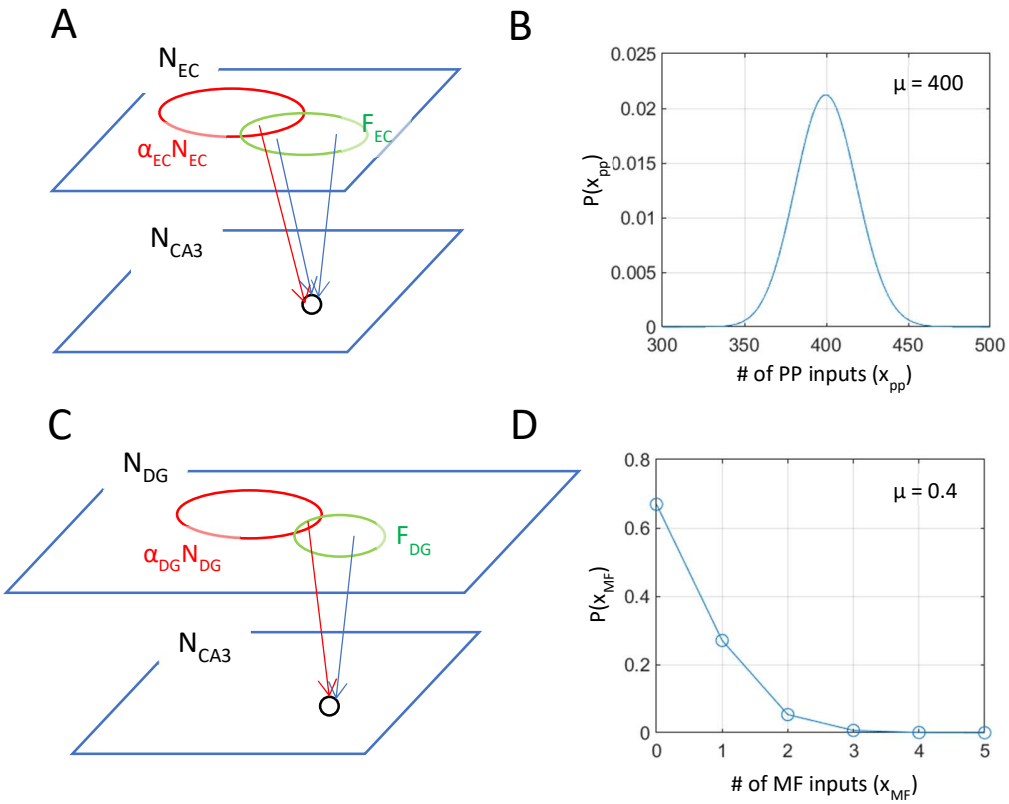


Figure D2, Probabilities for a CA3-PC to receive synaptic inputs from *x* number of presynaptic ensemble cells of the EC ($X_{pp}$, *A-B*) or those of the DG ($X_{MF}$, *C-D*) under the rat scale hippocampal network. The probabilities were calculated under the following conditions: Total number of principal cells in the EC ($N_{EC}$) = $2 \times 10^5$, and that in DG ($N_{DG}$) = $1 \times 10^6$; The number of synaptic inputs from the EC ($F_{EC}$) to a CA3-PC = 4000, and that from the DG ($F_{DG}$) = 40; The proportion of ensemble cells in the EC ($\alpha_{EC}$) = 10%, and that in the DG ($\alpha_{DG}$) = 1%.

*Appendix*

Assuming linear summation of EPSPs, the peak of sum of *k* EPSPs (ΣEPSP) that arrive every Δt within a time interval of T (Δt = T/k) can be calculated as follows:

$$\Sigma EPSP = J\{ A / [\exp(\Delta t/\tau_m) - 1]*[1-\exp(-k\Delta t/\tau_m)] - B /[\exp(\Delta t/\tau s)-1]*[1-\exp(-k\Delta t/\tau_s)] \}$$

, where $A = \exp((\Delta t - T_{peak})/\tau_m)$, $B = \exp((\Delta t - T_{peak})/\tau_s)$, and $T_{peak} = [\ln(1/\tau_m) - \ln(1/\tau_s)] / (1/\tau_m - 1/\tau_s)$. As *k* increases, ΣEPSP converges to

$$J\ (k\ \tau_m/T)\ \{\ \exp(-T_{peak}/\tau_m)\ [1 - \exp(-T/\tau_m)] -\ (\tau_s/\tau_m)\ \exp(-T_{peak}/\ \tau s)\ [1 - \exp(-T/\tau_s)]\ \}.$$

## References


1. Kowalski J, Gan J, Jonas P, Pernia-Andrade AJ. Intrinsic membrane properties determine hippocampal differential firing pattern in vivo in anesthetized rats. *Hippocampus* **26**, 668-682 (2016).

2. Guzman S, Schlögl A, Frotscher M, Jonas P. Synaptic mechanisms of pattern completion in the hippocampal CA3 network. *Science* **353**, 1117-1123 (2016).

3. Buzsáki G. Neural syntax: cell assemblies, synapsembles, and readers. *Neuron* **68**, 362-385 (2010).

4. Amaral DG, Ishizuka N, Claiborne B. Neurons, numbers and the hippocampal network. *Progress in Brain Research* **83**, 1-11 (1990).

5. Eom K*, et al.* Gradual decorrelation of CA3 ensembles associated with contextual discrimination learning is impaired by Kv1.2 insufficiency. *Hippocampus* **32**, 193-216 (2022).

6. Maurer AP*, et al.* Age-related changes in lateral entorhinal and CA3 neuron allocation predict poor performance on object discrimination. *Frontiers in Systems Neuroscience* **11**, 49 (2017).

7. O'Reilly RC, McClelland JL. Hippocampal conjunctive encoding, storage, and recall: avoiding a trade-off *Hippocampus* **4**, 661-682 (1994).

Supplementary Figure 1

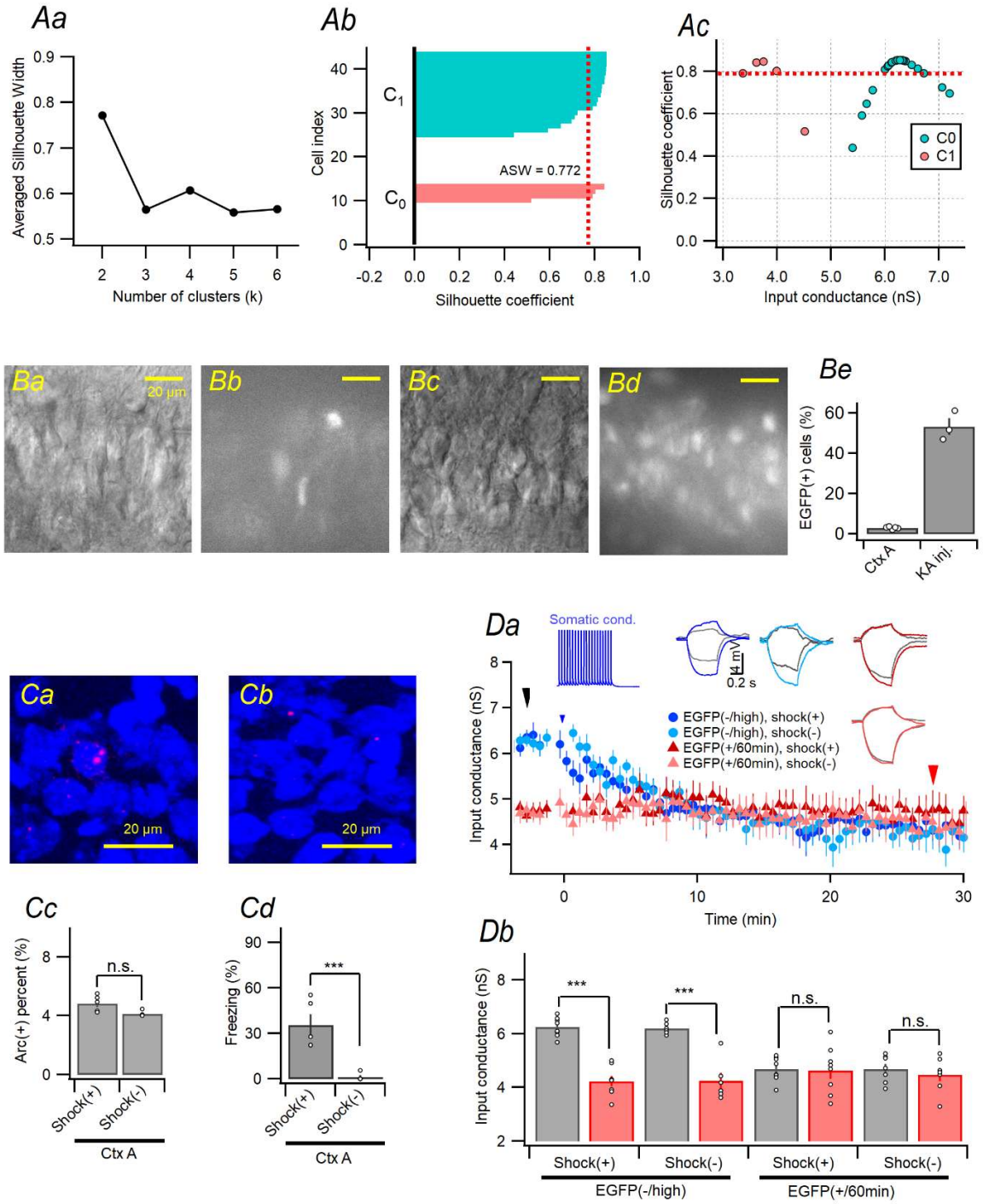

**Supplementary Figure 1.** **A**, Clustering of EGFP(-) neurons in figure 1. **Aa.** The maximal averaged silhouette width (ASW) of *k*-means clustering was found at k = 2, which means that EGFP(-) cells are optimally clustered into two subgroups. **Ab.** Silhouette coefficients of individual cells. The maximum ASW, 0.772, occurred at k = 2 [EGFP(-/high) = 20, EGFP(-/low) = 5]. **Ac.** Silhouette coefficients of individual cells as a function of their baseline $G_{in}$. **B.** To measure the infection efficiency in Figure 1, we induced a seizure by intraperitoneal injection of kainic acid (KA) under dox-free conditions two weeks after stereotaxic hippocampal injection of AAV-RAM-d2tTA-TRE-EGFP. One hour after the KA-induced seizure, we sacrificed the animals, and counted EGFP(+) and (-) CA3-PCs on the same focal plane of hippocampal slices under the epifluorescence imaging in combination with infrared-differential interference contrast (IR-DIC) imaging (Scalebar, 20 μm). The proportions of GFP(+) cells in the animals which visited a novel context (*Ba-Bb*) or experienced KA-induced seizure (*Bc-Bd*) was 3.00 ± 0.27 and 53.11 ± 4.17 %, respectively (bar graph in *Be*). These results suggest that the infection rate might be 50% assuming most CA3-PCs are activated under the KA-induced seizure. **C-D**. Animals were exposed to a novel context (context A) for 4 min. For shock(+) animals, but not for shock(-) animals, a single electrical shock was given at 3 min to a subset of the animals. **Ca-Cb.** Representative FISH images of Arc in the hippocampal CA3 area (red puncta) in either shocked (*Ca*) or non-shocked animals (*Cb*). **Cc.** Fraction of Arc(+) neurons in CA3 regions from shocked animals [shock(+), 5 animals, 4.84 ± 0.24%] or non-shocked animals [shock(-), 5 animals, 4.14 ± 0.10%]. **Cd.** Freezing behavior during the last one minute in context A of shocked (5 animals, 35.56 ± 7.16%) and non-shocked animals (5 animals, 1.39 ± 1.39%). **Da.** Baseline $G_{in}$ and post-conditioning $G_{in}$ changes of EGFP(-/high) and EGFP(+/60min) cells from shocked and non-shocked animals [denoted as shock(+) and shock(-), respectively]. The baseline $G_{in}$ and inducibility of LTP-IE did not differ between shocked and non-shocked groups. **Db.** Baseline $G_{in}$ (*gray bars*) and post-conditioning $G_{in}$ (*red bars*) of EGFP(-/high) and EGFP(+60min) neurons from shocked and non-shocked

animals [baseline *vs*. post-conditioning $G_{in}$ for EGFP(-/high) of shock(+), $p < 0.001$; EGFP(-/high) of shock(-), $p < 0.001$; EGFP(+/60min) of shock(+), $p = 0.878$; EGFP(+/60min) of shock(-), $p = 0.477$; LME model and simple effect analysis]. EGFP(-/high/shock+), $n = 8/8/6$; EGFP(-/high/shock-), $n = 6/6/4$; EGFP(+/60min/shock+), $n = 8/8/6$; EGFP(+/60min/shock-), $n = 7/7/5$; cell numbers ($n$) are indicated as numbers of cells/slices/animals.

## Supplementary Figure 2

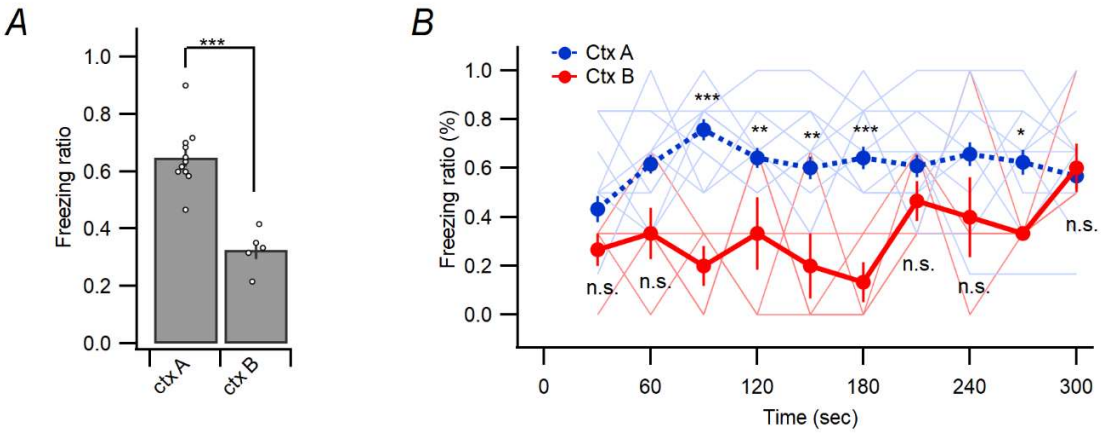


**Supplementary Figure 2.** **A**. Averaged freezing ratios elicited in context A and context B [$F_{(1,13.922)}$ = 29.603, p < 0.001; LME model]. Note that a standard contextual fear conditioning protocol (three days protocol of habituation-conditioning-retrieval steps) was used for the context A group, while the protocol of Fig. 2A or Fig. 3Ab was used for the context B group. As shown in the behavioral protocol for CtxAB in Figure 2A and 3Ab, animals visited to a novel context (context A) for 4 min 30 min before visiting context B. In context A, a single electrical shock (2 s, 0.7 mA) was given at 3 min. **B**. Mean freezing time course of animals measured in context B (*red thick line*, 5 animals) under the behavioral protocol of CtxAB mice shown in Figure 2A and 3Ab. For comparison, we displayed the freezing time course in context A of the animals, which experienced a single electrical shock in the same context once a day for three previous consecutive days (*Blue thick dotted line*, reproduced from Fig 3b1 of Eom et al., 2022)[20]. The freezing time courses of these two animal groups were significantly different from each other [Context: $F_{(1,127.187)}$ = 46.763, p < 0.001, LME model; 30 sec, p = 0.230; 60 sec, p = 0.054; 90 sec, p < 0.001; 120 sec, p = 0.009; 150 sec, p = 0.008; 180 sec, p < 0.001; 210 sec, p = 0.223; 240 sec, p = 0.150; 270 sec, p = 0.043; 300 sec, p = 0.771]. *Thin lines*, Freezing time courses of individual animals.

Supplementary Figure 3

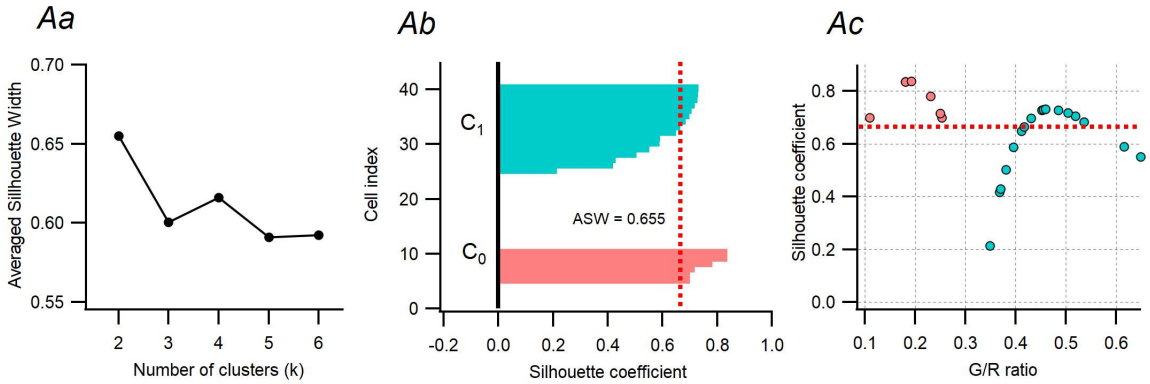


**Supplementary Figure 3.** *k*-means clustering of G/R ratio of ctxAB(++)neurons. **Aa.** The maximal averaged silhouette coefficient (ASW) occurred at k = 2, which means the optimal number of clustering. **Ab.** Silhouette coefficient of each cells. The maximum average silhouette width (ASW, 0.655) occurred at k = 2 [low G/R ratio = 7, high G/R ratio = 17]. **Ac.** Silhouette coefficient of each cells are plotted as a function of their baseline $G_{in}$. *Dotted lines*, mean value of ASW at k = 2.

Supplementary Figure 4

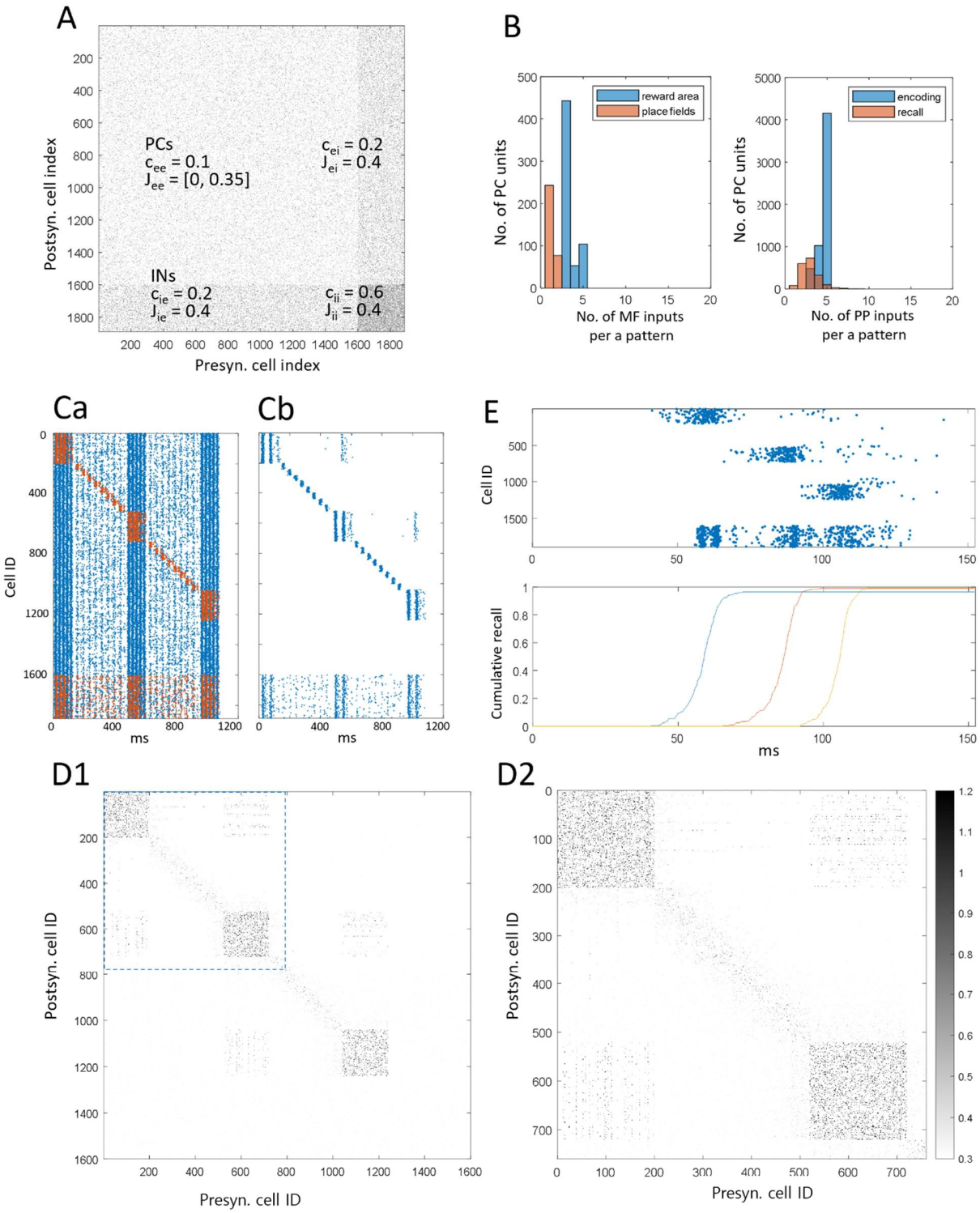

**Supplementary Figure 4.** Sequence learning of model CA3 network in the presence of place cell activation during inter-event intervals. **A**, Connectivity map between pyramidal cells (PCs, numbered by 1-1600) and interneurons (INs, 1601-1888). **B**, Distributions of the number of MF inputs (left) and PP inputs (right). MF and PP inputs to PCs in M subset (blue) during encoding phase followed the same lognormal distribution as Fig. 6Bb, but was limited to 5 instead of 15 to prevent overlap with inputs to the next place cells. MF inputs to place cells followed a lognormal distribution with $\mu = 0.5$ and $\sigma = 0.3$ but limited to 2 for the same reason (*red bars*, *left*). The PP inputs to M1 subset during the recall phase was the same as in Figure 6Bb. **C**, Raster plots for input patterns to the model CA3 network (*Ca*), and corresponding network responses to input patterns (*Cb*). Each of inter-event intervals were intervened by eight place fields, each of which recruited 40 place cells, which is one-fifth of an M subset size. MF and PP inputs to place cells and INs are indicated as red dots during inter-event intervals (*Ca*). Firing of place cells was largely governed by MF inputs. **D**, A matrix of A/C synaptic weights resulting from training the recurrent network using a patterns shown in *Ca*. The boxed area in *D1* is displayed in an expanded scale in *D2*. Green dots during the inter-event interval indicate weak potentiation of synaptic weights between place cells. **E**, Recall of the event sequence in the trained network. Applying weak PP inputs to M1 subset as shown in panel B (*red bars*) induced sequential activation of all three M subsets, but not the place cell trajectory.